ROMANIAN JOURNAL OF INFORMATION SCIENCE AND TECHNOLOGY
Volume **23**, Number S, pp. S67–S76, 2020

A Nonlinear Second-order Hyperbolic PDE-based Photon- limited Medical Microscopy Image Restoration Technique

Tudor Barbu
Institute of Computer Science, Romanian Academy –Iași Branch
tudor.barbu@iit.academiaromana-is.ro

Abstract. A novel partial differential equation (PDE) – based denoising framework for photon-limited medical microscopy images is proposed in this article. Such a microscopy image processing approach could be further applied in the analysis of the medical images of viruses and bacteria, thus being useful in the context of the current coronavirus pandemic. The considered technique is based on a nonlinear hyperbolic second-order PDE model. The differential model is then solved numerically by applying a consistent and fast converging finite difference-based iterative approximation algorithm to it. The numerical approximation scheme provided here removes successfully the Poisson noise from the microscopy images representing viruses like COVID-19, while enhancing their essential details and thus facilitating their analysis. Quantum denoising experiments and method comparison results are also described.

Keywords: Medical informatics for epidemics, photon-limited microscopy image, quantum noise, nonlinear hyperbolic second-order PDE model, finite difference-based method, numerical approximation algorithm.

1. Introduction

Microscopy imaging, which covers the use of microscope image processing and analysis techniques [1], has taken a very important role in domains like medicine and biological research. It helps visualize the miscroscopic world and detect and investigate the causative agents of infectious diseases, such as various viruses and bacteria. Depending on the type of the miscroscope used for the image aquisition process, various microscopy imaging solutions, including the electron miscroscopy, fluorescence microscopy and confocal microscopy have been developed.

Unfortunately, the acquisition devices may generate various types of noise in the medical images. While they are most often affected by the well-known *additive white Gaussian noise* (AWGN) [2], the occurrence of other types of noise in medical imaging represents also a concern.

The *quantum*, or *shot*, *noise* damages the captured images both quantitatively and qualitatively, generating the *photon-limited images*. It is also called *Poisson noise*, since it is characterized by the following Poisson distribution: $P(n) = \frac{e^{-\mu}\mu^n}{n!}, n \geq 0$ [3].

This noise is generated by the imaging acquisition mechanisms based on photon-counting devices. Such devices, which capture the images by counting the photon detections at various spatial locations over a certain period of observation and produce the Poisson noise, are used by some medical imaging procedures, like the single photon emission computed tomography, the positron-emission tomography, and the confocal, electron and fluorescence microscopy imaging processes [4, 5]. Since the quantum noise occurs in medical images because of the arrival of photons to the sensors that are independent of each other, the shot denoising task is a quite difficult one.

Various Poisson denoising solutions have been proposed in the last years. The conventional nonlinear image filters, like the 2D median filter [2], are used to remove the quantum noise, but they could also affect the boundaries or other features.

More powerful quantum noise filtering methods that have been introduced include the Poisson Reducing Bilateral Filter – PRBF [6], the Non-Local Mean – NLM Poisson filter [7], the Multi Scale Variance Stabilizing Transform (MS-VST) [8], the moving average filter, the Minimum Description Length (MDL) – based scheme [9], and the Wavelet-based [10] and the Platelet-based algorithms [11]. These restoration techniques work quite well for photon-limited medical images [4].

Another important category of effective photon-limited image restoration approaches is that of the variational and partial differential equation (PDE) – based quantum denoising models. The variational and non-variational PDE schemes of second and fourth order have been used successfully for image restoration in the last 35 years. Some effective nonlinear PDE-based Poisson denoising solutions have been derived from the nonlinear PDE-based white additive Gaussian noise removal techniques [12]. We mention here the variational shot denoising methods based on the total variation (TV) regularization [13, 14].

We have proposed many PDE-based image restoration techniques in the last years [15-17]. In this paper we also consider an effective nonlinear PDE-based Poisson noise removal technique that restores the photon-limited microscope images while preserving their details and overcoming the unintended effects. The proposed microscopy image processing approach removes successfully the quantum noise from medical images representing pathogen agents and enhances their essential features. So, it could facilitate the further microscopy image analysis process that detects and investigates the entities from those microscope images, thus being useful in the fight against current coronavirus pandemic [18]. It is based on a nonlinear hyperbolic second-order partial differential equation with boundary conditions that is described in the following section.

An iterative fast converging finite difference-based approximation algorithm that solves numerically the proposed PDE model is constructed in the third section. The numerical discretization scheme is then successfully applied in our filtering experiments performed on microscope images representing COVID-19 viruses [18], which are described in the fourth section. The conclusions of this research work are drawn in the last section.

2. Nonlinear Second-order Hyperbolic PDE Model

The proposed Poisson denoising framework for medical images is based on the following differential model, which is composed of the next nonlinear second-order hyperbolic PDE and several boundary conditions:

$$\begin{cases} \lambda \dfrac{\partial^2 u}{\partial t^2} + \xi \dfrac{\partial u}{\partial t} - \beta \varphi\left(\left\|\nabla^2 u\right\|\right) div\left(\psi\left(\left\|\nabla u\right\|\right)\nabla u\right) + \alpha\left(\dfrac{u-u_0}{|u|+\delta}\right) = 0 \\ u(x,y,0) = u_0(x,y), \quad \forall (x,y) \in \Omega \subseteq R^2 \\ u_t(x,y,0) = u_1(x,y), \quad \forall (x,y) \in \Omega \\ u(x,y,t) = 0, \quad \forall\ (x,y) \in \partial\Omega \\ \dfrac{\partial u}{\partial \vec{n}}(x,y,t) = 0, \quad \forall (x,y) \in \partial\Omega \end{cases} \tag{1}$$

where $\alpha, \beta, \lambda, \xi, \delta \in (0,1]$, $\Omega \subseteq R^2$ is the image domain and $u_0 \in L^2(\Omega)$ represents the observed photon-limited image.

The proposed diffusivity function of this nonlinear PDE-based model has the following form:

$$\psi : [0,\infty) \to [0,\infty), \psi(s) = \left(\frac{\eta}{\left|\zeta s^k + \gamma \log 10(\eta)\right|}\right)^{\frac{1}{k-1}} \tag{2}$$

where its parameters are $\zeta \in (0,1]$, $\gamma \in (0.5,1]$, $k \geq 3$ and $\eta \geq 20$. It is properly constructed for an effective diffusion-based denoising process [13-15], since it is monotonically decreasing and converges to 0.

The component $div\left(\psi\left(\left\|\nabla u\right\|\right)\nabla u\right)$ performs the diffusion along the image edges and not across them [12, 15, 16], so overcoming the blurring, while the component $\varphi\left(\left\|\nabla^2 u\right\|\right)$ controls the speed of this diffusion process and is based on the following positive function:

$$\varphi : [0,\infty) \to [0,\infty), \varphi(s) = \frac{1}{\varepsilon}\left(\nu s^{r-1} + \varsigma\right)^{\frac{1}{r}} \tag{3}$$

where $\varepsilon, \nu, \varsigma, r \in [1,5)$.

The second-time derivative $\dfrac{\partial^2 u}{\partial t^2}$, which provides the hyperbolic character of this nonlinear PDE denoising model, is sharpening the edges, thus enhancing the image details. The last term of the PDE, $\alpha\left(\dfrac{u-u_0}{|u|+\delta}\right)$, is encouraging the similarity to the observed image, being also related to the Poison distribution [3].

While the PDE-based model (1) is non-variational, since it does not result from the minimization of any energy cost functional, it is well-posed, admitting a unique variational (weak) solution. A finite difference-based numerical approximation algorithm that solves the proposed hyperbolic PDE model and converges to that solution is constructed in the next section.

3. Numerical Approximation Scheme

We apply the finite-difference method to solve the considered nonlinear PDE-based model [19]. A grid of space size h and the time step Δt is constructed first, by quantizing the space coordinates as $x = ih, y = jh, i \in \{1,\ldots, I\}$, $j \in \{1,\ldots, J\}$ and the time coordinate as $t = n\Delta t$, where the dimension of the support image is $[Ih \times Jh]$.

The partial differential equation in (1) can be re-written as follows:

$$\lambda \frac{\partial^2 u}{\partial t^2} + \xi \frac{\partial u}{\partial t} + \alpha \left(\frac{u - u_0}{|u| + \delta} \right) = \beta \varphi \left(\left\| \nabla^2 u \right\| \right) div \left(\psi \left(\left\| \nabla u \right\| \right) \nabla u \right) \quad (4)$$

The left term of (4) is then discretized, by applying the central differences [19], as following:

$$\begin{aligned} &\lambda \frac{u_{i,j}^{n+\Delta t} + u_{i,j}^{n-\Delta t} - 2u_{i,j}^{n}}{\Delta t^2} + \xi \frac{u_{i,j}^{n+\Delta t} - u_{i,j}^{n-\Delta t}}{2\Delta t} + \alpha \left(\frac{u_{i,j}^{n} - u_{i,j}^{0}}{\left| u_{i,j}^{n} \right| + \delta} \right) = u_{i,j}^{n+\Delta t} \left(\frac{\lambda}{\Delta t^2} + \frac{\xi}{2\Delta t} \right) + \\ &+ u_{i,j}^{n-\Delta t} \left(\frac{\lambda}{\Delta t^2} - \frac{\xi}{2\Delta t} \right) + u_{i,j}^{n} \left(\frac{\alpha}{\left| u_{i,j}^{n} \right| + \delta} - \frac{2\lambda}{\Delta t^2} \right) - u_{i,j}^{0} \frac{\alpha}{\left| u_{i,j}^{n} \right| + \delta} \end{aligned} \quad (5)$$

and leads to $u_{i,j}^{n+1} \left(\frac{2\lambda + \xi}{2} \right) + u_{i,j}^{n-1} \left(\frac{2\lambda - \xi}{2} \right) + u_{i,j}^{n} \left(\frac{\alpha}{\left| u_{i,j}^{n} \right| + \delta} - 2\lambda \right) - u_{i,j}^{0} \frac{\alpha}{\left| u_{i,j}^{n} \right| + \delta}$ for $\Delta t = 1$.

The right term in (4) is approximated next. First, $\varphi \left(\left\| \nabla^2 u \right\| \right)$ is discretized as $\varphi \left(\frac{u_{i+h,j}^{n} + u_{i-h,j}^{n} + u_{i,j+h}^{n} + u_{i,j-h}^{n} - 4u_{i,j}}{h^2} \right)$. Then, the divergence term $div \left(\psi \left(\left\| \nabla u \right\| \right) \nabla u \right)$ is approximated as $\frac{1}{4} \begin{bmatrix} \psi \left(\left\| u_{i+h,j}^{n} - u_{i,j}^{n} \right\| \right) \left(u_{i+h,j}^{n} - u_{i,j}^{n} \right) + \psi \left(\left\| u_{i-h,j}^{n} - u_{i,j}^{n} \right\| \right) \left(u_{i-h,j}^{n} - u_{i,j}^{n} \right) + \\ + \psi \left(\left\| u_{i,j+h}^{n} - u_{i,j}^{n} \right\| \right) \left(u_{i,j+h}^{n} - u_{i,j}^{n} \right) + \psi \left(\left\| u_{i,j-h}^{n} - u_{i,j}^{n} \right\| \right) \left(u_{i,j-h}^{n} - u_{i,j}^{n} \right) \end{bmatrix}$.

If we consider h = 1, the following explicit numerical approximation scheme is obtained:

$$u_{i,j}^{n+1}\left(\frac{2\lambda+\xi}{2}\right)=u_{i,j}^{n}\left(2\lambda-\frac{\alpha}{\left|u_{i,j}^{n}\right|+\delta}\right)+u_{i,j}^{n-1}\left(\frac{\xi-2\lambda}{2}\right)+u_{i,j}^{0}\frac{\alpha}{\left|u_{i,j}^{n}\right|+\delta}+$$
$$\beta\frac{\varphi\left(u_{i+1,j}^{n}+u_{i-1,j}^{n}+u_{i,j+1}^{n}+u_{i,j-1}^{n}-4u_{i,j}\right)}{4}\left[\begin{array}{l}\psi\left(\left\|u_{i+1,j}^{n}-u_{i,j}^{n}\right\|\right)\left(u_{i+1,j}^{n}-u_{i,j}^{n}\right)+\psi\left(\left\|u_{i-1,j}^{n}-u_{i,j}^{n}\right\|\right)\left(u_{i-1,j}^{n}-u_{i,j}^{n}\right)+\\+\psi\left(\left\|u_{i,j+1}^{n}-u_{i,j}^{n}\right\|\right)\left(u_{i,j+1}^{n}-u_{i,j}^{n}\right)+\psi\left(\left\|u_{i,j-1}^{n}-u_{i,j}^{n}\right\|\right)\left(u_{i,j-1}^{n}-u_{i,j}^{n}\right)\end{array}\right] \quad (6)$$

The explicit iterative finite difference-based numerical approximation algorithm given by (6) is consistent to the PDE model (1) and converges fast to its weak solution representing the restored photon-limited image that is u^{N+1}. This numerical scheme has been used successfully in our quantum denoising experiments, which are discussed in the following section.

4. Experiments and Method Comparison

The proposed nonlinear hyperbolic PDE-based Poisson denoising framework has been successfully tested on hundreds of photon-limited medical images. The most restoration experiments have been performed on the microscope image collections of the Public Health Image Library (PHIL) of the Centers for Disease Control and Prevention [18].

That PHIL database, which contains several thousands of images, is available at https://phil.cdc.gov and its collections can be accessed via the links or using keywords in the search boxes on that site. We have used 75 microscope COVID-19 images and also 65 electron microscopy images of EM Imagery collection representing other viruses and bacteria, from the PHIL database, in our experiments.

These numerical simulations have been performed on an Intel (R) Core (TM) i7-6700HQ CPU 2.60 GHz processor on 64 bits, operating Windows 10. The MATLAB programming environment has been used for the implementation of the presented numerical algorithm.

The iterative numerical algorithm described in the last section filters properly the quantum noise, overcomes the undesired effects, such as image blurring and staircasing, and preserves and even enhances the essential details like boundaries, corners and other features. Since it converges fast to the solution of the PDE model, representing the recovered image, the number of iterations *N* is quite low, therefore the running time is short enough, of ony a few seconds. However, the required number of processing steps and the execution time depend much on the dimension of the photon-limited image and the amount of the shot noise.

The performance of the proposed Poisson denoising technique has been assessed using various similarity metrics [20]. Thus, we have used the PSNR (Peak Signal to Noise Ratio), computed as the ratio between the maximum possible value of an image and the power of the noise that corrupts that image and measured in decibels (dB), the SNR (Signal to Noise Ratio) and the MSE (Mean-Squared Error), representing average squared difference between the image and its noisy version.

The above-mentioned 140 test images from the PHIL database have been used as references for these similarity measures. They have been corrupted with various levels of Poisson noise and the PSNR, SNR and MSE values have been computed for all those photon-limited images. Then, the average values of these performance measures, based on all these experiments, have been determined.

The performance of this technique depends also on a proper selection of the parameters of this model in the equations (1) - (3). Their optimal values have been determined empirically, by using the trial and error method, as those providing the best average PSNR, SNR and MSE values. We have obtained optimal restoration results for the parameter values $k = 3$, $\eta = 30$ and $r = 2$. Also, the parameter δ should take very low values, like $\delta < 0.1$. The intervals specified for the other model's coefficients in the second section are properly chosen for an optimal Poisson denoising.

Satisfactory method comparison results have been achieved. Thus, the restoration method described here outperforms both the conventional denoising models, such as the two-dimensional median filter, and some second-order PDE-based filtering approaches, like the total variation (TV) – based schemes adapted for quantum noise, since it provides better values for those mentioned performance measures and also executes somewhat faster.

As the values in the following table show, the proposed nonlinear second-order hyperbolic PDE-based restoration framework has achieved better average values of the three performance measures than other Poisson denoising algorithms, such as the 2D Median filter, the TV-based quantum denoising scheme, the Bilateral 2D filter and the NLM filter. That means higher PSNR and SNR average values, but lower MSE average values.

Table 1. Average PSNR, MSE and SNR values for some shot denoising models

Restoration technique	**Average PSNR**	**Average MSE**	**Average SNR**
The proposed approach	33.3697 (dB)	29.9301	33.0576
Median filter	28.8361 (dB)	85.0093	28.2003
Bilateral 2D filter	29.2061 (dB)	78.0666	28.6433
TV-based Poisson denoising	30.8756 (dB)	60.5191	30.3135
NLM filter	31.7068 (dB)	43.8936	31.3238

Some examples from our numerous medical image denoising simulations are described in the following figures. The medical images in Fig. 1 (a) and Fig. 2 (a) are provided by National Institute of Allergy and Infectious Diseases (NIAID) and, like all the images from the PHIL database, belong to the public domain and thus are free of any copyright restrictions. They are acquired by using electron microscopes, describe MERS - CoV viral particles, and are corrupted by some amounts of quantum noise.

These photon-limited COVID-19 - related images are filtered of Poisson noise by applying the proposed nonlinear PDE-based technique and the output achieved by our approach after $N = 25$ iterations is displayed in (b), in both figures. The Total Variation - based Poisson denoising results produced after 40 filtering steps are depicted in (c). The two-dimension Median filtering output is displayed in the (d) images, while the restoration results provided by the Bilateral and the NLM two-dimension filters, are described in (e) and (f) respectively.

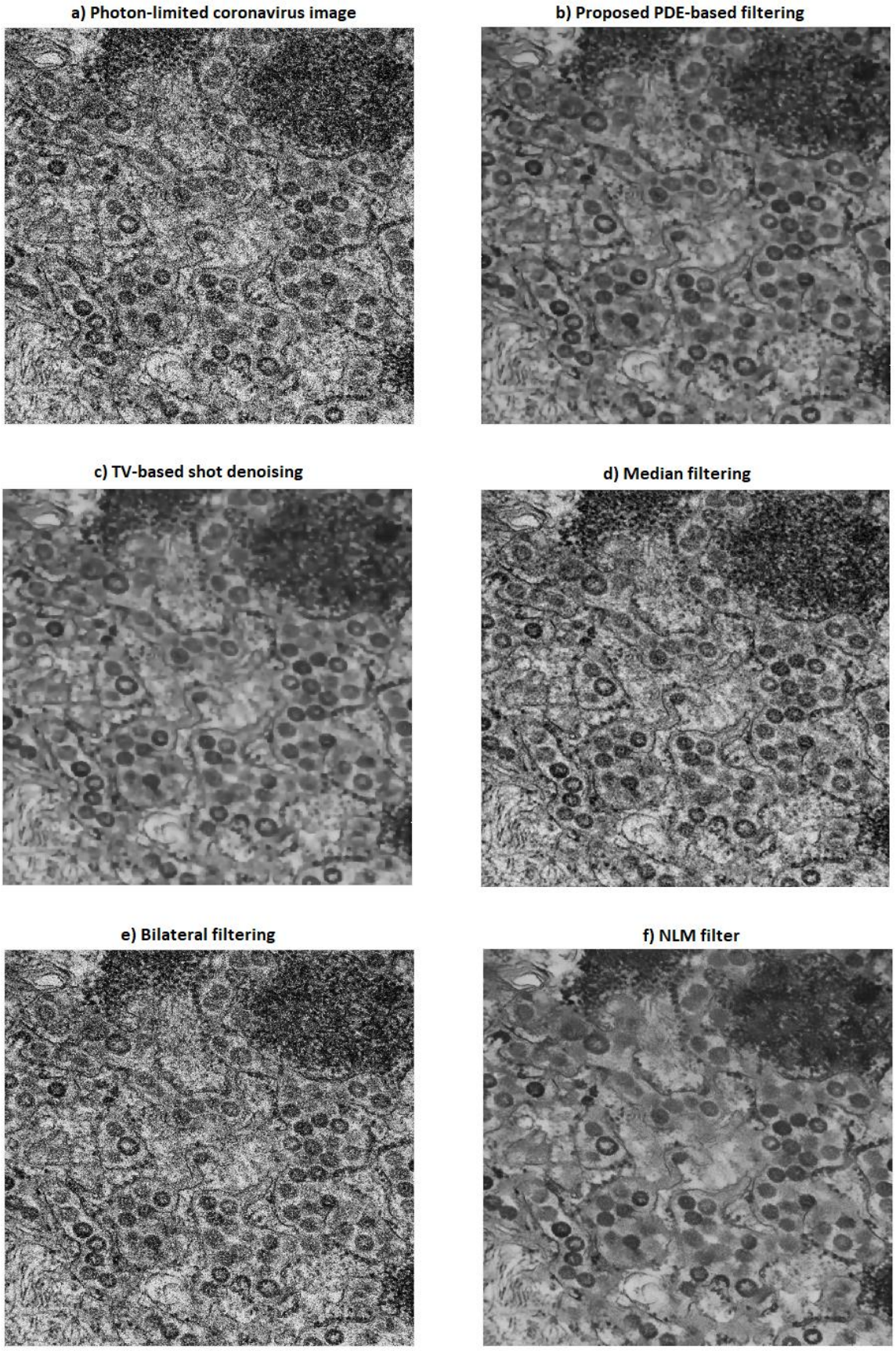

Fig. 1 Photon-limited electron microscope image restored by various methods

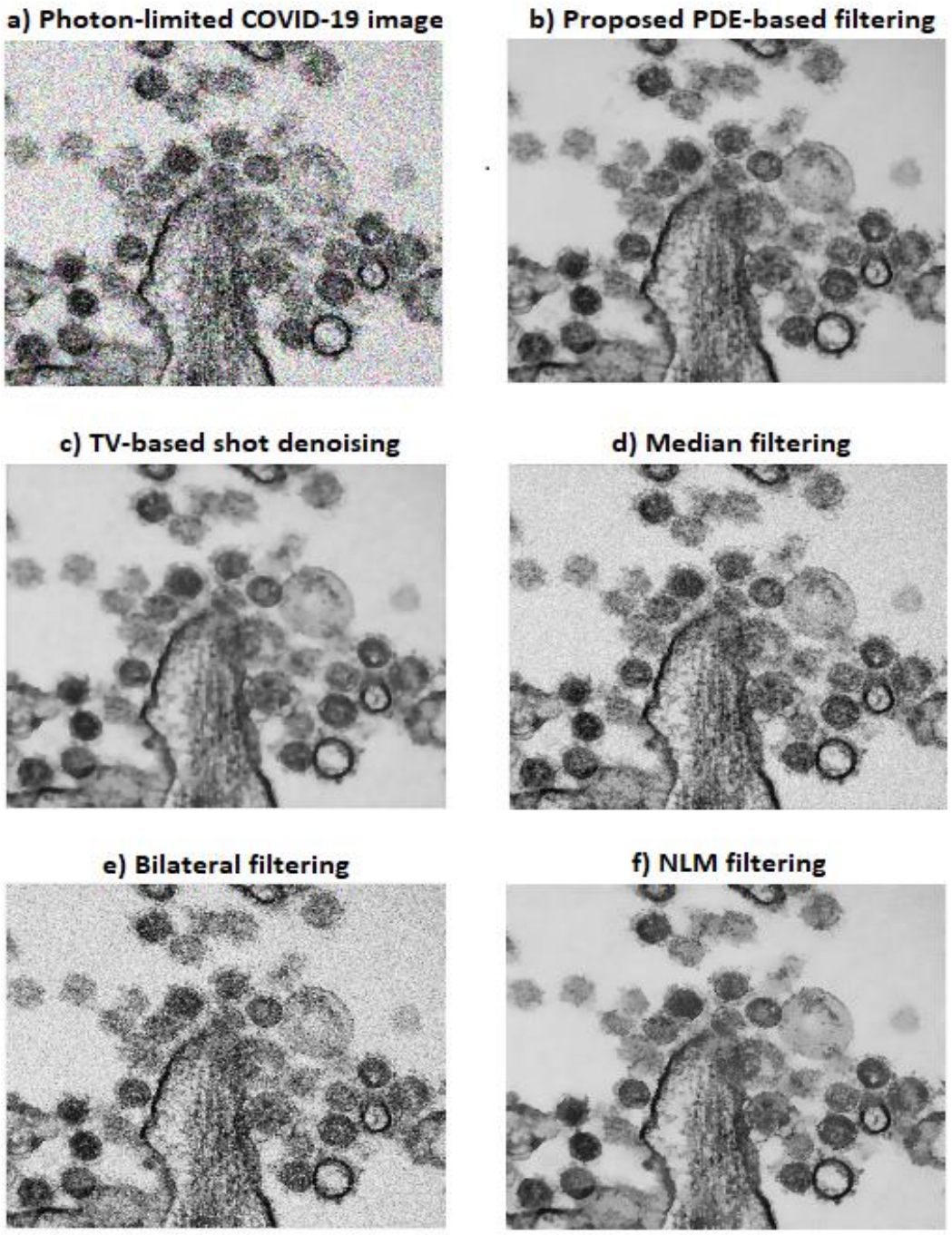

Fig. 2 Photon-limited COVID-related microscope image filtered by various methods

These figures illustrate that the shot denoising results obtained by the hyperbolic PDE scheme proposed here have a better quality (as the PSNR, SNR and MSE values in Table 1 also show) and are also produced quite faster than the restored versions achieved by other Poisson noise removal methods, such as TV Poisson denoising, since the proposed technique requires fewer processing iterations. The viral entities could be more easily detected in the coronavirus images filtered by our method. That means it would lead to better microscopy image visualization and analysis, and a better medical diagnosis and treatment.

5. Conclusions

We have described a novel second-order nonlinear hyperbolic PDE-based photon-limited restoration technique that removes successfully the Poisson noise generated by the acquisition equipment, from medical images such as those generated by electron or confocal microscopes that are based on photon detection. The proposed filtering framework overcomes also the unintended effects, and, given the hyperbolic character of its differential model, it preserves and sharpens the edges and other details of the processed image.

The enhancement of those essential details of the medical images is important for any medical imaging task. Such a filtering and feature enhancement technique can be further applied in the image-based medical diagnosis and treatment domains. We have applied the developed quantum noise filtering technique in the microscopy imaging domain, on medical images related to the current coronavirus pandemic. It could lead to a good microscope image analysis and medical diagnosis in this domain.

The nonlinear partial differential equation-based model that is proposed here represents the main contribution of this research work. It is well-posed, and unlike the most existing PDE-based shot denoising schemes, it has a hyperbolic and non-variational character.

The fast converging finite difference method-based numerical approximation algorithm constructed here is another contribution of this paper. The numerical scheme is stable and consistent to the differential model and has been successfully applied in the COVID-19 image restoration experiments performed by us. The described numerical simulations illustrate the effectiveness of the considered photon-limited PDE-based restoration approach that outperforms some state of the art quantum denoising techniques.

Acknowledgements. The author is grateful to the anonymous referees for their very constructive remarks and suggestions.

Conflict of Interest. The author of this manuscript declare that he has no conflict of interest.

References

[1] BONNET N., *Some trends in microscope image processing*, Micron, vol. 35, no. 8, 2004, pp. 645–654.

[2] GONZALES R., WOODS, R., *Digital image processing*, Prentice Hall, New York, NY, USA, 2nd edition, 2001.

[3] HAIGHT F. A., *Handbook of the Poisson distribution*, New York: John Wiley & Sons, 1967.

[4] RODRIGUES I., SANCHES J., BIOUCAS_DIAS J., *Denoising of medical images corrupted by poisson noise*, 15th IEEE International Conference on Image Processing, ICIP 2008, 2008, pp. 1756–1759.

[5] KERVRANN C., SORZANO C. O. S., ACTON S. T., OLIVO-MARIN J. -C., UNSER M., *A guided tour of selected image processing and analysis methods for fluorescence and electron microscopy*, IEEE Journal of Selected Topics in Signal Processing 10 (1), 2016, pp. 6-30.

[6] THAKUR K. V., DAMODARE O. H., SAPKAI A. M., *Poisson noise reducing bilateral filter*, Procedia Computer Science, 79, 2016, pp. 861–865.

[7] BUADES A., COLL B., MOREL J. M., *A review of image denoising algorithms, with a new one*, Multiscale Model. Simul. 4 (2), 2005, pp. 490–530.

[8] ZHANG B., FADILLI, J. M., STARCK J. L., *Multi-scale variance stabilizing transform for multi-dimensional Poisson count image denoising*, Proceedings of IEEE ICASSP '2006, Toulouse, France, 2006.

[9] NOWAK R. D., FIGUEIREDO M. A. T., *Unsupervised progressive parsing of poisson fields using minimum description length criteria*, Proceedings of International Conference on Image Processing, ICIP 99, vol. 2, 1999, pp. 26–30.

[10] UNSER M., ALDROUBI A., LAINE A., *Guest editorial: wavelets in medical imaging*, IEEE Transactions on Medical Imaging, vol. 22, no. 3, 2003, pp. 285–288.
[11] WILLETT R. M., NOWAK R. D., *Fast multiresolution photon-limited image reconstruction*, IEEE International Symposium on Biomedical Imaging: Nano to Macro, Volume 2, 15-18 April 2004, pp. 1192–1195.
[12] WEICKERT J., *Anisotropic diffusion in image processing*, European Consortium for Mathematics in Industry. B. G. Teubner, Stuttgart, Germany, 1998.
[13] ABERGEL R., LOUCHET C., MOISAN L., ZENG T., *Total variation restoration of images corrupted by Poisson noise with iterated conditional expectations*, Scale Space and Variational Methods in Computer Vision, Springer International Publishing, 2015, pp. 178-190.
[14] SAWATZKY A., BRUNE C., MULLER J., BURGER M., *Total variation processing of images with poisson statistics*, Computer Analysis of Images and Patterns, Springer, 2009, pp. 533–540.
[15] BARBU T., *Nonlinear PDE model for image restoration using second-order hyperbolic equations*, Numerical Functional Analysis and Optimization, Volume 36, Issue 11, Taylor & Francis, 2015, pp. 1375-1387.
[16] BARBU T., FAVINI A., *Rigorous mathematical investigation of a nonlinear anisotropic diffusion-based image restoration model*, Electronic Journal of Differential Equations, Volume 2014, Issue 129, 2014, pp. 1-9.
[17] BARBU T., *Second-order anisotropic diffusion-based technique for Poisson noise removal*, IFAC PapersOnLine, Elsevier Ltd., Volume 52, Issue 18, 2019, pp. 174-178.
[18] *Interim clinical guidance for management of patients with confirmed coronavirus disease (COVID-19*). Centers for Disease Control and Prevention, https://www.cdc.gov/coronavirus/2019-ncov/hcp/clinical-guidance-management-patients.html, 6 April 2020.
[19] JOHNSON P., *Finite difference for PDEs*, School of Mathematics, University of Manchester, Semester I, 2008.
[20] THUNG K. - H., RAVEENDRAN P., *A survey of image quality measures*, International Conference for Technical Postgraduates (TECHPOS), Kuala Lumpur, Malaysia, December 2009, pp. 1-4.